

PAPER • OPEN ACCESS

Evaluation of porosity in 3D printed trabecular bone structures for prostheses

To cite this article: I Buj *et al* 2021 *IOP Conf. Ser.: Mater. Sci. Eng.* **1193** 012038

View the [article online](#) for updates and enhancements.

You may also like

- [Monte Carlo investigation into feasibility and dosimetry of flat flattening filter free beams](#)
Sergei Zavgorodni
- [IPEM topical report 1: guidance on implementing flattening filter free \(FFF\) radiotherapy](#)
Geoff Budgell, Kirstie Brown, Jason Cashmore et al.
- [An analytical formalism to calculate phantom scatter factors for flattening filter free \(FFF\) mode photon beams](#)
Heeteak Chung, Karl L Prado and Byong Yong Yi



The Electrochemical Society
Advancing solid state & electrochemical science & technology

242nd ECS Meeting

Oct 9 – 13, 2022 • Atlanta, GA, US

Abstract submission deadline: **April 8, 2022**

Connect. Engage. Champion. Empower. Accelerate.

MOVE SCIENCE FORWARD



Submit your abstract



Evaluation of porosity in 3D printed trabecular bone structures for prostheses

I Buj^{1*}, A Bagheri¹, M Ferrer², A Domínguez¹

¹ Department of Mechanical Engineering. School of Engineering of Barcelona (ETSEIB), Av. Diagonal, 647. 08028, Barcelona, Spain

² Department of Strength of Materials and Structural Engineering. School of Engineering of Barcelona (ETSEIB), Av. Diagonal, 647. 08028, Barcelona, Spain

*Corresponding author: irene.buj@upc.edu

Abstract: Hip prostheses require an external porous area in order to fix them by means of osseointegration. Different structures can be printed in order to favour bone fixation, such as octet-truss or trabecular, among others. In the present paper, bone-like structures are printed in cubic shapes, by means of fused filament fabrication (FFF). Three design parameters of the structures were varied: the number of joining points per unit volume, the area scale and the offset that is given to the different struts of the structure. Both the theoretical and the measured porosity of the samples is evaluated, from the drawing of the structures and by means of weight measurements respectively. As expected, the structures having fewer union points per unit volume are more porous than the structures having more points. When low number of points generating struts of the structure were employed, measured porosity is lower than the theoretical one, while when high number of points is considered, the opposite situation is found. The present work will help to obtain porous structures to be used in prostheses, by means of extrusion 3D printing processes.

Keywords: 3D printing, Voronoi structure, FFF, FDM.

1. Introduction

In recent years, 3D printing processes have undergone an important development [1]. ISO/ASTM 52900 standard [2] divides the additive manufacturing (AM) processes into seven different categories: 1-VAT polymerisation, 2-material jetting, 3-binder jetting, 4-material extrusion, 5-powder bed fusion, 6-sheet lamination and 7-direct energy deposition. One of the most employed extrusion printing process is fused filament fabrication (FFF), also known as fused deposition modelling (FDM). It allows printing complex structures from a melted plastic filament by layer upon layer deposition in a cheap way [3]. Different plastic materials can be printed with the FFF technology, such as polylactic acid (PLA), polyethylene terephthalate (PET-G), acrylonitrile butadiene styrene (ABS), etc. However, dimensional accuracy and surface finish are not especially good in this case.

In order to ensure the fixation of prostheses by means of bone growth and osseointegration, the prostheses require porous structures [4,5]. The requirements for the porous area consist of total porosity between 50 and 90 % [6] and pore size between 100 μm and 500 μm [7]. In addition, surface area and interconnectivity of the pores are related to permeability, which governs nutrient transport, and mechanical strength of the structures, among other properties [8]. In order to mimic the trabecular structure of bones, in a previous work, a trabecular structure was designed and printed from a



Content from this work may be used under the terms of the [Creative Commons Attribution 3.0 licence](https://creativecommons.org/licenses/by/3.0/). Any further distribution of this work must maintain attribution to the author(s) and the title of the work, journal citation and DOI.

geometrical model [3]. In the present work, an alternative trabecular structure is presented that is developed from a Voronoi structure.

2. Materials and methods

2.1. Design of the samples

First, cubic samples of size $20 \times 20 \times 20$ mm were designed with the help of the Rhinoceros software and its plug-in, Grasshopper (figure 1(1)). To generate the bone-like structure using the "Population 3D" command, a set of points was distributed in the created cubic space (figure 1(2)). These points were randomly inserted in the cubic volume. Then, utilizing the Voronoi 3D command, a set of 3D Voronoi was formed all over the cubic volume, in which all obtained Voronoi 3D geometries were merged (figure 1(3)). Afterwards, the 3D Voronoi parts were separated. For doing this, the "Explode block" command was employed (figure 1(4)). Then, the Explode command was applied to break points, edges, and faces in the 3D Voronoi cells to allow equidistant copy of the faces to create polyhedron cells separated each other an equivalent distance to bone trabecular thickness (figure 1(5)). Area canvas was selected in all the surfaces of Voronoi, and using "Explode" canvas the chosen area was removed (figure 1(6)). Next, by means of the "Point" command all the points were selected (figure 1(7)), and employing the Mesh quad, the quadratic mesh was applied on the geometry (figure 1(8)). Finally, this structure was further improved with Weaverbird command, a plugin for Grasshopper software, with the Catmull-Clark smoothing command, which softened the trabecular mesh model (figure 1(9)).

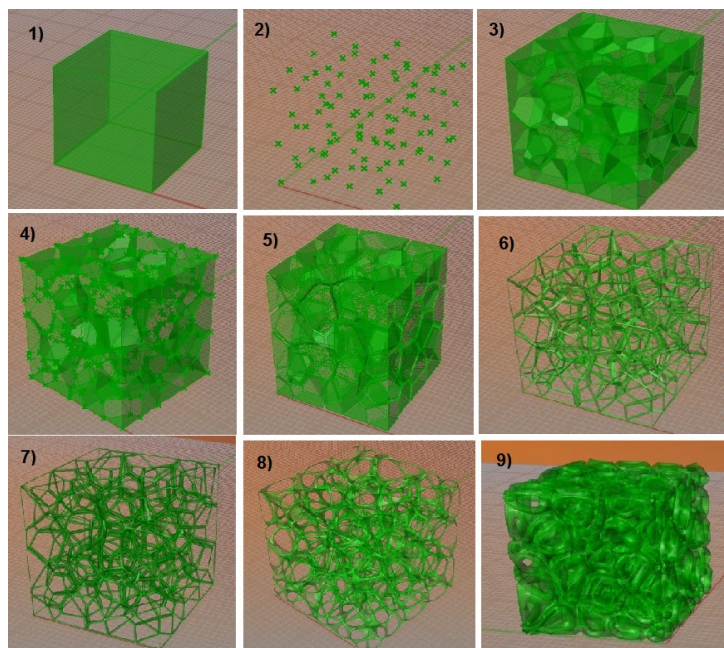


Figure 1. Design of the Voronoi cubic samples.

After designing the structures, it was observed that they were difficult to be printed, because of their thin walls (figure 2). Thus, their design was modified in order to have thicker walls (see figure 3).

In order to increase and adequately the appropriate thickness of the struts the Meshmixer software was employed. The nozzle size to print the specimens was selected 0.3 mm. The wall thickness should not be less than two times of the nozzle diameter. Therefore, to achieve the suitable walls the minimum thickness was set to be 0.7 mm. According to this selection, the geometry was simulated on the Meshmixer and then final improved structure was created.

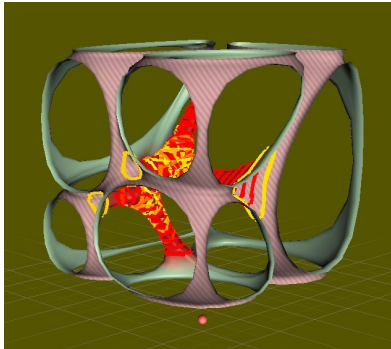


Figure 2. Initial design of the samples.

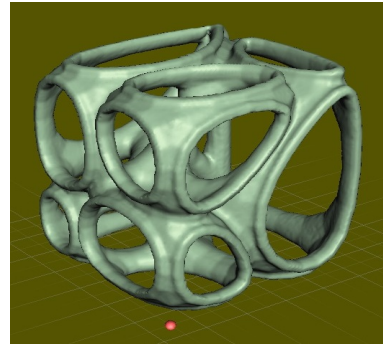


Figure 3. Final design of the samples.

2.2. Printing process of the samples

White PLA filament of 2.85 mm diameter was used, from BCN3D. The cubic samples were printed in a Sigma R19 printer from BCN3D. Printing parameters are presented in table 1.

Table 1. Printing parameters.

Parameter	Value
Printing speed (mm/s)	40
Nozzle diameter (mm)	0.3
Layer height (mm)	0.1
Printing infill (%)	100

Soluble polyvinyl alcohol (PVA) supports were employed to print the samples, which were removed after the printing operation.

Table 2. Variables of the DOE.

Variable	Units
Number of points per unit volume (PU)	Points/mm ³
Area scale factor (AS)	-
Offset (OF)	mm

2.3. Experimental design

A two-level factorial design of experiments (DOE) was defined with three levels (2^3). Selected variables are presented in table 2.

The number of points generating struts within a certain volume of the structure enables the distribution of the struts randomly all over the volume. Then, with respect to this points each Voronoi cell is formed. The area scale factor allows to control the size of each face of the Voronoi cell. When each area of the Voronoi cell increases the width of the Voronoi edge is decreases. On the other hand, the higher the area scale, the lower the thickness of each edge (figure 2(6)). In addition, utilizing the offset the strut size of the bone-like structure is defined, to obtain desirable porosity and pore size of the bone-like structure. By increasing the offset the wall thickness of the Voronoi cell's side increases, whereas pores and porosity decrease. On contrary, the reduction of wall thickness by decreasing the offset leads to the increment of the porosity and pore size. It means that the higher offset, the lower the porosity and pore size (figure 2(5)).

2.4. Determination of porosity

Theoretical porosity of the structures was determined from the Solid Works drawing using the

Meshmixer software. Experimental porosity of the samples was calculated from their weight, considering the dimensions of the cubes and the plastic density. A Kern 440-33N scale was used, with a precision of 0.01 g.

3. Results

The summarized porosity results are presented in table 3.

Table 3. Results.

Experiment	PU (points/mm ³)	AS	OF (mm)	Theoretical porosity (%)	Measured porosity (%)
1	3	0.938	0.821	88.9	83.82
2	97	0.938	0.821	49.6	53.73
3	3	0.955	0.821	88.1	86.15
4	97	0.955	0.821	49.5	50.99
5	3	0.938	0.865	87.1	83.69
6	97	0.938	0.865	48.4	54.18
7	3	0.955	0.865	88.4	85.56
8	97	0.955	0.865	48.7	51.75

Highest porosity value of 88.9 % corresponds to low number of points, low area scale and low offset. Lowest porosity value of 48.4 % corresponds to high number of points, high area scale and high offset. As a general trend, when low number of points per unit volume is used, measured porosity is lower than the theoretical one. On the contrary, for high number of points per unit volume, measured porosity is higher than the theoretical one.

The simplified regression model for Theoretical porosity, with R²-adj of 99.94 % is presented in equation (1). The interactions are not significant in this model.

$$\text{Theoretical porosity (\%)} = 106.14 - 0.41569 \text{ PU} - 19.89 \text{ OF} \quad (1)$$

Figure 4 depicts a contour plot for Theoretical porosity as a function of offset distance and number of points per unit volume.

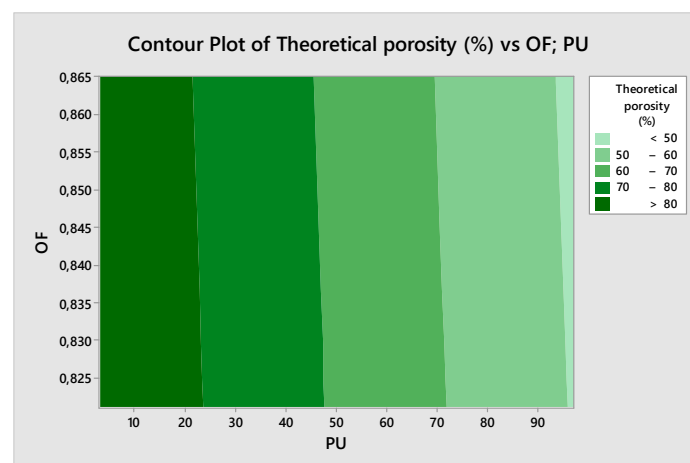


Figure 4. Contour plot of Theoretical porosity vs OF; PU.

It can be observed that the higher the number of points the lower porosity is, with a slight effect of offset distance employed.

The simplified regression model for Measured porosity, with R^2 -adj of 99.35 % is presented in equation (2). The interactions are not significant in this model.

$$\text{Measured porosity (\%)} = 85.831 - 0.3419 \text{ PU} \quad (2)$$

Figure 5 shows the contour plot for Measured porosity as a function of offset distance and number of points per unit volume.

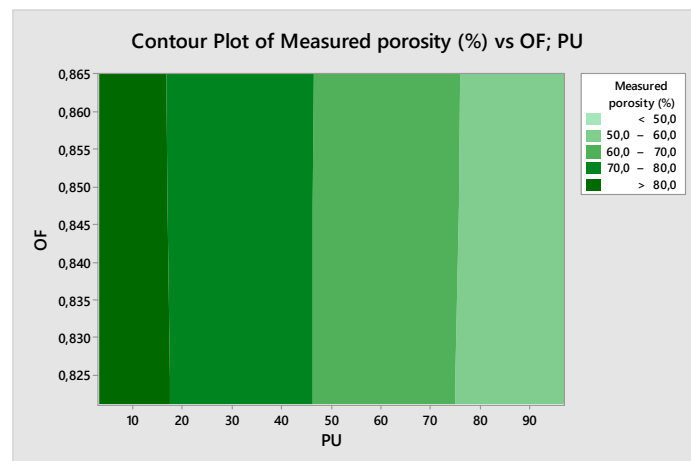


Figure 5. Contour plot of Measured porosity vs OF; PU.

Measured porosity increases with the number of points per unit volume, regardless of selected offset value. As an example, figure 6 shows a printed cubic sample with the trabecular structure.

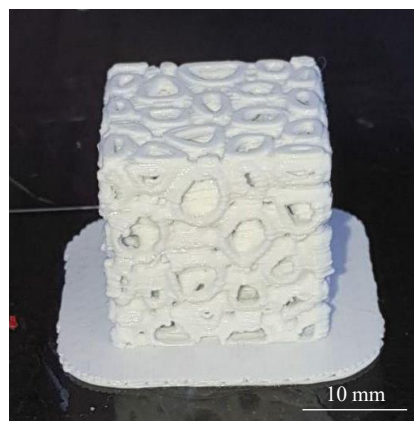


Figure 6. Example of a printed sample.

4. Conclusions

In the present work, bone-like structures obtained from a Voronoi structure were designed and printed. Their porosity was determined both theoretically and by means of weight measurement. The main conclusions are as follows:

- Porosity decreases when the number of points in the considered space, while it decreases slightly with offset.
- The area scale does not show an important effect on porosity.

- When low number of points is considered measured porosity is lower than the theoretical one. On the contrary, when high number of points is considered, measured porosity is higher than the theoretical one.

In the future, the modulus of elasticity for the structure would be compared both analytically and experimentally. The present work will help to mimic porous tissues such as the trabecular structures of bones by means of the FFF processes.

Acknowledgements

The authors wish to acknowledge Ramón Casado-López for his help with the experimental tests. This project was co-financed by the European Union Regional Development Fund within the framework of the ERDF Operational Program of Catalonia 2014-2020 with a grant of 50% of total cost eligible, project BASE3D, grant number 001-P-001646.

References

- [1] Gibson I, Rosen D and Stucker B. Additive Manufacturing Technologies. 3D printing, Rapid Prototyping and Direct Digital Manufacturing 2015 p 459 Springer Boston, MA
- [2] ISO/ASTM 52900-2015 *Standard Terminology for Additive Manufacturing – General Principles – Terminology*. International Standard Organization / American Society for Testing and Materials
- [3] Buj-Corral I, Bagheri A and Petit-Rojo O 2018 3D Printing of Porous Scaffolds with Controlled Porosity and Pore Size Values *Materials* **11** (9) p 1532
- [4] Buj-Corral I, Tejo A and Fenollosa F 2020 Development of AM technologies for metals in the sector of medical implants *Metals* **10** (5) p 686
- [5] Stanciu AM, Sprecher CM, Adrien J, Roiban LI, Alini M, Gremillard L and Peroglio M 2018 Robocast zirconia-toughened alumina scaffolds: Processing, structural characterisation and interaction with human primary osteoblasts. *Journal of the European Ceramic Society* **38** (3) pp 845-853
- [6] Salgado A J, Coutinho O P and Reis R L 2004, Bone Tissue Engineering: State of the Art and Future Trends *Macromolecular Bioscience* **4** pp 743-765
- [7] Karageorgiou V and Kaplan D 2005 Porosity of 3D biomaterial scaffolds and osteogenesis *Biomaterials* **26** pp 5474–5491
- [8] Egan P F, Sheal K A and Ferguson S J 2018 Simulated tissue growth for 3D printed scaffolds *Biomechanics and Modeling in Mechanobiology* **17** (5) pp 1481-1495